

University of Groningen

A minimal sensing and communication control strategy for adaptive platooning

Yang, Kang; Liu, Di; Yu, Wenwu

Published in:
International Journal of Adaptive Control and Signal Processing

DOI:
[10.1002/acs.3255](https://doi.org/10.1002/acs.3255)

IMPORTANT NOTE: You are advised to consult the publisher's version (publisher's PDF) if you wish to cite from it. Please check the document version below.

Document Version
Publisher's PDF, also known as Version of record

Publication date:
2022

[Link to publication in University of Groningen/UMCG research database](#)

Citation for published version (APA):

Yang, K., Liu, D., & Yu, W. (2022). A minimal sensing and communication control strategy for adaptive platooning. *International Journal of Adaptive Control and Signal Processing*, 36(2), 373-390.
<https://doi.org/10.1002/acs.3255>

Copyright

Other than for strictly personal use, it is not permitted to download or to forward/distribute the text or part of it without the consent of the author(s) and/or copyright holder(s), unless the work is under an open content license (like Creative Commons).

The publication may also be distributed here under the terms of Article 25fa of the Dutch Copyright Act, indicated by the "Taverne" license. More information can be found on the University of Groningen website: <https://www.rug.nl/library/open-access/self-archiving-pure/taverne-amendment>.

Take-down policy

If you believe that this document breaches copyright please contact us providing details, and we will remove access to the work immediately and investigate your claim.

Downloaded from the University of Groningen/UMCG research database (Pure): <http://www.rug.nl/research/portal>. For technical reasons the number of authors shown on this cover page is limited to 10 maximum.

A minimal sensing and communication control strategy for adaptive platooning

Kang Yang¹  | Di Liu^{1,2} | Wenwu Yu^{1,3} 

¹School of Cyber Science and Engineering, Southeast University, Nanjing, China

²Bernoulli Institute for Mathematics, Computer Science and Artificial Intelligence, University of Groningen, Groningen, the Netherlands

³School of Mathematics, Southeast University, Nanjing, China

Correspondence

Wenwu Yu, School of Mathematics, Southeast University, Nanjing 210096, China.

Email: wwyu@seu.edu.cn

Funding information

Jiangsu Provincial Key Lab of Networked Collective Intelligence, Grant/Award Number: BM2017002; National Natural Science Foundation of China, Grant/Award Numbers: 61673107, 62073074, 62073076

Summary

Several cooperative driving strategies proposed in literature, sometimes known as cooperative adaptive cruise control strategies, assume that both relative spacing and relative velocity with preceding vehicle are available from on-board sensors (laser or radar). Alternatively, these strategies assume communication of both velocity states and acceleration inputs from preceding vehicle. However, in practice, on-board sensors can only measure relative spacing with preceding vehicle (since getting relative velocity requires additional filtering algorithms); also, reducing the number of variables communicated from preceding vehicle is crucial to save bandwidth. In this work we show that, after framing the cooperative driving task as a distributed model reference adaptive control problem, the platooning task can be achieved in a minimal sensing and communication scenario, that is, by removing relative velocity measurements with preceding vehicle and by removing communication from preceding vehicle of velocity states. In the framework we propose, vehicle parametric uncertainty is taken into account by appropriately designed adaptive laws. The proposed framework is illustrated and shown to be flexible to several standard architectures used in cooperative driving (one-vehicle look-ahead topology, leader-to-all topology, multivehicle look-ahead topology).

KEYWORDS

cooperative driving, distributed adaptation, minimal sensing and communication, model reference adaptive control

1 | INTRODUCTION

Intelligent transportation and autonomous vehicles¹ have been attracting increasing research interests because of the potential to reduce congestion, improve the traffic safety and decrease carbon emissions.^{2,3} Studies have shown that groups of vehicles driving at small intervehicle distances (i.e., grouped into platoons) can lead to reduced air drag and promote energy savings.^{4,5} However, vehicle-following functionalities with small intervehicle distances pose the so-called string stability problem,^{6,7} which refers to the problem of how such small intervehicle distances can be maintained throughout the platoon even in the presence of disturbances. Adaptive cruise control (ACC)⁸ was one of the first technologies studied for vehicle-following functionality with one-vehicle look-ahead topology. The idea is that on-board sensors (laser or radar) can measure relative spacing with the preceding vehicle (or calculate relative velocity after appropriate filtering) and use this information to automatically accelerate or brake. Despite

ACC technology is now widely available in commercial vehicles, it is not recommended to use it to form platoons, since this technology can be unsafe in the sense of string stability in commercial applications: for example, the authors of Reference 9 experimentally find that ACC systems can guarantee string stability only for large enough time headway (time headway larger than 0.8 s in their work); recently, also the authors of Reference 10 find that commercial ACC systems can exhibit string unstable features. Therefore, for small enough time headways, any disturbance in ACC-equipped platoons will cause intervehicle distances to increase throughout of the platoon. Based on these issues, improvements to standard ACC have been the object of deep investigation. One of the most promising findings was that ACC systems can achieve better performance by enhancing on-board sensors with wireless communication from preceding vehicle: this vehicle-to-vehicle communication can provide measurements that cannot be obtained from on-board sensors, most notably, acceleration from preceding vehicle. In the presence of such additional information, this ACC system with vehicle-to-vehicle communication was called cooperative adaptive cruise control (CACC) system.^{11,12}

A number of studies have analyzed the string stability properties of CACC,^{13,14} showing improved performance of CACC in this sense.^{3,15-17} Several communication topologies have been studied: for example, Reference 18 shows that string stability of the vehicle platoon can be achieved by implementing a CACC communication structure with leading vehicle speed and acceleration information broadcast along the platoon. However, it was also shown that wireless communication can be highly unreliable and subject to strong network-induced constraints. The research presented in this work takes the steps from the challenges of CACC systems. A first challenge is that CACC strategies proposed in literature typically assume that both relative spacing and relative velocity with preceding vehicle are available from on-board sensors. Otherwise, they assume that velocity from preceding vehicle can be communicated together with acceleration input (double communication channel). The same sensing and communication also extends to adaptive cooperative driving strategies, where vehicle parametric uncertainty is taken into account. However, in practice the on-board sensors can only obtain relative spacing with preceding vehicle, since getting relative velocity requires additional filtering algorithms: at the same time, it is fundamental to reduce as much as possible communication channels from preceding vehicle in order to save bandwidth and prevent as much as possible the aforementioned network-induced constraints. Note that standard CACC architectures exist beyond the one-vehicle look-ahead topology, mainly the leader-to-all topology and multivehicle look-ahead topology. Because the radar/laser can only measure the relative position with the preceding vehicle (it is impossible to use on-board sensors to measure directly the relative distance of the second preceding vehicle, the third preceding vehicle, and so forth), it is mandatory for these topologies to communicate the relative positions among vehicles. Therefore, a minimal communication scenario seems to be the one where the preceding vehicle only communicates its own acceleration input and, for topologies beyond the one-vehicle look-ahead, also relative spacing from other vehicles.

In this work we want to show that, after framing the cooperative driving task as a distributed model reference adaptive control (MRAC) problem, the platooning task can be achieved in a minimal sensing and communication scenario. The term “minimal sensing and communication scenario” refers to the fact that of removing relative velocity measurements with preceding vehicle and removing communication of velocity states from preceding vehicle (in one-vehicle look-ahead topology). The proposed framework is illustrated not only for one-vehicle look-ahead topology, but it is flexible to the other standard architectures used in cooperative driving such as leader-to-all topology and multivehicle look-ahead topology (in these cases, the preceding vehicle must necessarily communicate the relative spacing from other preceding vehicles). Being based on MRAC, an important aspect of the proposed CACC strategy is its capability of dealing with uncertain vehicle dynamics, which can be even heterogeneous¹⁹ in nature. In reality, vehicles on the road are all different and with uncertain dynamics. There can be great differences in their engine dynamics.²⁰⁻²² A study conducted in Reference 23 showed the causes of heterogeneity of vehicles in a platoon and their effects on string stability; Reference 6 studies the string stability of nonlinear bidirectional asymmetric heterogeneous platoon systems; a distributed adaptive sliding mode controller is derived in Reference 24 to guarantees string stability and adaptive compensation of disturbances based on constant spacing policy for a heterogeneous vehicle platoon; the heterogeneous string stability is studied with unidirectional interconnected MIMO systems in Reference 25.

Because we frame the cooperative driving task as a distributed MRAC problem, it is worth mentioning that this work extends and improves approaches proposed in recent years, in which synchronization problems have been described as a special MRAC.^{20,26} In these approaches, each agent tries to match the model of the leading vehicle or of their neighbors by using “feedback matching gains” or “coupling matching gains”.²⁷⁻²⁹ As compared with this literature, the main contribution of this work can be listed as follows:

- Design the proposed adaptation laws for the feedback matching gains and coupling matching gains in a control scenario with relative degree two,
- Achieving the platooning task in a minimal sensing and communication scenario, that is, by removing velocity measurements and communication of velocity states (in one-vehicle look-ahead topology),
- Showing flexibility to other standard architectures used in CACC, namely, leader-to-all topology and multivehicle look-ahead topology.

Simulations on a platoon of 4 + 1 vehicles (four followers and one reference model that places the role of leader) are conducted to validate the theoretical analysis. A recent work distributed on MRAC is Reference 30. With respect to this, we consider systems of relative degree two, and is also provide the solutions to the matching conditions in a closed form. We believe that both points are relevant since vehicle models have relative degree greater or equal to two, while the closed form solutions to the distributed matching conditions have not appeared before in the platooning literature. It is worth acknowledging that alternative architectures exist for synchronizing heterogeneous vehicles, which however have never found (yet) a direct application in actual CACC protocols. One such method is the so-called distributed observer method^{31,32} in which the observation of the leader state is communicated among neighbors. A possible reason why this alternative architecture has not found a direct application in actual CACC protocols is that it requires more communication effort (in order to communicate the variables of the distributed observer). Therefore, such an architecture will not be covered in this work. Using a minimal sensing and communication scenario as we study can promote robustness of the platooning task, for example, because the approach can be less affected by communication impairments.

The rest of the article is organized as follows: the platooning model is presented in Section 2; the different communication topologies addressed in this work are in Section 3; the adaptive protocol are designed in Section 4. Simulations are provided in Section 5 with conclusions in Section 6.

2 | PLATOONING MODEL

Consider a heterogeneous platoon with M vehicles, where the term “heterogeneous” refers to the fact that for any two vehicles i, j with dynamics (in transfer function form)

$$y_i = G_i(s)u_i = k_i \frac{1}{s(s + \tau_i)} u_i, \quad (1)$$

$$y_j = G_j(s)u_j = k_j \frac{1}{s(s + \tau_j)} u_j, \quad (2)$$

the parameters k_i, k_j and τ_i, τ_j might differ from each other. In (1) and (2), $u_i, u_j \in \mathbb{R}$, and $y_i, y_j \in \mathbb{R}$ are inputs and outputs of the two vehicles, respectively. τ_i, τ_j are unknown positive parameters, and k_i, k_j are positive high-frequency constants.

Remark 1. The model (1), (2) can be interpreted as follows. Assume each vehicle is acceleration-controlled without low-level control: then u_i, u_j are the acceleration directly provided to the vehicles, and the time constants τ_i, τ_j will be zero or close to zero. In this case, the model (1), (2) would be a second-order integrator that is often considered in cooperative control. Another (more practical) interpretation of (1), (2) is: assume that each vehicle is velocity-controlled with a low-level controller to track a desired velocity: then u_i, u_j are the desired velocities provided to the low-level control, and the time constants τ_i, τ_j represent the time constant of the low-level control. It is also worth mentioning that sometimes the literature assumes that each vehicle is acceleration-controlled with a low-level controller to track a desired acceleration: in this case, one would have a double integrator $\frac{1}{s^2}$ in (1), (2) in place of $\frac{1}{s}$: u_i, u_j would be the desired acceleration provided to the low-level control, and the time constants τ_i, τ_j represent the time constant of the low-level control. However, such a model is not considered in this work, because it results in a system with relative degree 3, requiring a completely different control design. Addressing this model can be the object of future work.

In (1), (2), the vehicles are indexed as 1, 2, ..., M : the index 0 is reserved for a reference model. The dynamics of vehicle 0 can be expressed (in transfer function form) as:

$$y_0 = G_0(s)r = k_0 \frac{1}{s^2 + a_1s + a_0} r, \quad (3)$$

where $r \in \mathbb{R}$ is the model reference input, $y_0 \in \mathbb{R}$ is the model reference output, and k_0 is the high-frequency gain. In (3), a_1, a_0 are design parameters such that the polynomial $s^2 + a_1s + a_0$ is stable, that is, $a_1, a_0 > 0$. In other words, (3) represents the desired response of the leader to a change in the reference input: this is in line with the celebrated model reference control approach.

The main task of each vehicle is to maintain the required distance from the preceding vehicle. To achieve this goal, we use a constant distance headway spacing policy to denote the required distance r_{ji} between vehicle i and j

$$e_{ji} = y_j - y_i + r_{ji}, \quad (4)$$

the control objective is to adjust e_{ji} to zero for all vehicles in the platoon. Without loss of generality, we take $r_{ji} = 0$ since the case $r_{ji} \neq 0$ can be treated via a coordinate transformation.

In the rest of the article we will mainly follow a notation stemming from MRAC.³³ It is well known that the vehicle i can be synchronized to the reference model (3) by using a control law with the following structure:

$$u_i = l_i^* \frac{1}{s + \lambda_0} u_i + f_i^* \frac{1}{s + \lambda_0} y_i + g_i^* y_i + c_i^* r, \quad (5)$$

where $\lambda_0 > 0$ such that the filter in (5) is stable, and $l_i^*, f_i^*, g_i^*, c_i^*$ are control gains. The control law (5) can be interpreted as a combination of feedback/feedforward (the first three terms are the feedback parts and the last one is a feedforward term). The term ‘‘synchronized to the reference model’’ refers to the fact that the closed-loop transfer function of vehicle i should match the transfer function of the reference model (3). This matching problem can be solved under the following assumptions:

- (R1) $s^2 + a_1s + a_0$ is a monic Hurwitz polynomial,
- (R2) the relative degree of $G_0(s)$ is equal to 2, the same as that of $G_i(s)$,
- (A1) an upper bound of the degree of $s(s + \tau_i)$ is known, that is, it is $n = 2$,
- (A2) the sign of the high-frequency gain k_i is known, that is, it is positive.

These assumptions are all verified for (1)–(3). Therefore, the scalars l_i^*, f_i^*, g_i^* , and c_i^* are well defined and they can be found by solving the following matching problem

$$\frac{c_i^* k_i}{s(s + \tau_i)[(s + \lambda_0) - l_i^*] - k_i[f_i^* + g_i^*(s + \lambda_0)]} = \frac{k_0}{(s^2 + a_1s + a_0)(s + \lambda_0)}. \quad (6)$$

Similar to chapter 5 in Reference 33, the matching conditions for vehicle i to the reference model can be defined as follows

$$\begin{aligned} c_i^* k_i &= k_0, \\ s(s + \tau_i)[(s + \lambda_0) - l_i^*] - k_i[f_i^* + g_i^*(s + \lambda_0)] &= (s^2 + a_1s + a_0)(s + \lambda_0). \end{aligned} \quad (7)$$

By direct calculation of (7), it is not difficult to get

$$\begin{aligned} l_i^* &= \tau_i - a_1, \\ f_i^* &= \frac{\tau_i - \tau_i^2 + a_1\tau_i - a_0 - a_1\lambda_0}{k_i}, \\ g_i^* &= \frac{\tau_i^2\lambda_0 - \tau_i\lambda_0 + a_1\lambda_0}{k_i}, \\ c_i^* &= \frac{k_0}{k_i}. \end{aligned} \quad (8)$$

However, because the parameters of vehicle i are unknown, the proposed control law (5) cannot be used for vehicle i . Therefore, it is necessary to propose a new control law to adapt to the unknown parameters, which will be discussed in Section 4.

In addition, in line with recent results in Reference 26, we also discuss the problem of matching the dynamics of vehicle i to the dynamics of vehicle j . This is useful when vehicle j is not directly connected to the leading vehicle and thus can only synchronize to the neighboring vehicle.

Proposition 1. *There exists an ideal control law that can match the vehicle j to vehicle i , and its form is as follows*

$$u_j = l_{ji}^* \frac{1}{(s + \lambda_0)} u_i + f_{ji}^* \frac{1}{(s + \lambda_0)} y_i + g_{ji}^* y_i + c_{ji}^* u_i + l_j^* \frac{1}{(s + \lambda_0)} (u_j - u_i) + f_j^* \frac{1}{(s + \lambda_0)} (y_j - y_i) + g_j^* (y_j - y_i), \quad (9)$$

and the gains l_{ji}^* , f_{ji}^* , g_{ji}^* satisfy the following matching conditions

$$s(s + \tau_j)[(s + \lambda_0) - (\bar{l}_j^* - \bar{l}_{ji}^*)] - k_j[(f_j^* - f_{ji}^*) + (s + \lambda_0)(g_j^* - g_{ji}^*)] = (s + \lambda_0)(s^2 + a_1 s + a_0), \quad (10)$$

where $c_{ji}^* = \frac{k_i}{k_j}$, $\bar{l}_{ji}^* = \frac{l_{ji}^*}{c_{ji}^*}$, and $\bar{l}_j^* = \frac{l_j^*}{c_{ji}^*}$.

Proof. First, let us rewrite the control law (9)

$$u_j = \frac{(l_{ji}^* - l_j^*)u_i + (f_{ji}^* - f_j^*)y_i + (s + \lambda_0)(g_{ji}^* - g_j^*)y_i + l_j^* y_j + g_j^* y_j (s + \lambda_0) + c_{ji} u_i (s + \lambda_0)}{(s + \lambda_0) - l_j^*}, \quad (11)$$

substitute the control law (11) into (2) and use the following matching conditions of vehicle j to the reference model

$$s(s + \tau_j)[(s + \lambda_0) - l_j^*] - k_j[f_j^* + (s + \lambda_0)g_j^*] = (s^2 + a_1 s + a_0)(s + \lambda_0), \quad (12)$$

which leads to

$$\begin{aligned} & [(s + \lambda_0)(s^2 + a_1 s + a_0)](y_j - y_i) + \{s(s + \tau_j)[(s + \lambda_0) - l_j^*] - k_j[f_{ji}^* + (s + \lambda_0)g_{ji}^*]\}y_i \\ &= k_j s(s + \tau_j) c_{ji}^* \left((s + \lambda_0) + \frac{l_{ji}^*}{c_{ji}^*} - \frac{l_j^*}{c_{ji}^*} \right) u_i. \end{aligned} \quad (13)$$

then (13) can be written as

$$s(s + \tau_j) \left((s + \lambda_0) - (\bar{l}_j^* - \bar{l}_{ji}^*) \right) - k_j \left((f_j^* - f_{ji}^*) + (s + \lambda_0)(g_j^* - g_{ji}^*) \right) = (s + \lambda_0)(s^2 + a_1 s + a_0) \quad (14)$$

with $c_{ji}^* = \frac{k_i}{k_j}$, $\bar{l}_{ji}^* = \frac{l_{ji}^*}{c_{ji}^*}$, and $\bar{l}_j^* = \frac{l_j^*}{c_{ji}^*}$. This completes the proof. ■

Remark 2. Proposition 1 shows a distributed matching condition among neighboring vehicles. In other words, there exist gains that match an agent to its neighbors. Such distributed matching condition has been derived without extra assumptions.

By direct solution of (10), it is not difficult to see that

$$\begin{aligned} l_{ji}^* &= (c_{ji}^* - 1)a_1 + (1 - c_{ji}^*)\tau_j, \\ f_{ji}^* &= \tau_j - \lambda_0 \tau_j, \\ g_{ji}^* &= a_1 \lambda_0 \tau_j. \end{aligned} \quad (15)$$

Remark 3. Note that, in case of homogeneous vehicles ($k_i = k_j \forall i, j$ and $\tau_i = \tau_j \forall i, j$), one has $c_{ji}^* = 1$ and therefore $l_{ji}^* = 0$. This implies that this coupling should not be estimated. In addition, in case of homogeneous and acceleration-controlled vehicles ($k_i = k_j \forall i, j$ and $\tau_i = \tau_j = 0 \forall i, j$) it is easy to find that (8) and (15) simplify to

$$\begin{aligned} l_i^* &= -a_1, & f_i^* &= \frac{-a_0 - a_1 \lambda_0}{k_i}, & g_i^* &= \frac{a_1 \lambda_0}{k_i}, \\ l_{ji}^* &= 0, & f_{ji}^* &= 0, & g_{ji}^* &= 0. \end{aligned} \quad (16)$$

However, because the parameters of vehicles i and j are unknown, the proposed control law (9) cannot be used for vehicle j . Therefore, it is necessary to propose a new control law to adapt to the unknown parameters, which will be discussed in Section 4.

3 | COMMUNICATION TOPOLOGIES

In this work, we consider a platoon of vehicles that are linked to each other via a communication graph that describes the allowed information flow. The communication graph is composed of nodes (i.e., vehicle) and directed edges (i.e., communication links). In other words, vehicle i has a directed connection to vehicle j if j can receive information from i . The communication graph describing the allowed information flow among all the vehicles, is completely defined by the pair $\mathcal{G} = (\mathcal{V}, \mathcal{E})$, where $\mathcal{V} = \{1, \dots, N\}$ is a finite nonempty set of nodes, and $\mathcal{E} \subseteq \mathcal{V} \times \mathcal{V}$ is a set of pairs of nodes, called edges. To include the presence of leader vehicle (vehicle 0) in the platoon we define $\bar{\mathcal{G}} = \{\mathcal{V}, \mathcal{E}, \mathcal{T}\}$, where $\mathcal{T} \subseteq \mathcal{V}$ is the set of those vehicles, called target vehicles, which receive information from the leader vehicle.

We consider a platoon of four vehicles, which will be used also in our simulation studies. Figure 1(A) provides a simple communication graph describing a classic one-vehicle look-ahead topology where $\mathcal{V} = \{1, 2, 3, 4\}$, $\mathcal{E} = \{(1, 2), (2, 3), (3, 4)\}$ and $\mathcal{T} = \{1\}$. Let us introduce the adjacency matrix $\mathcal{A} = [a_{ij}] \in \mathbb{R}^{N \times N}$ of a directed communication, which is defined as $a_{ii} = 0$ and $a_{ij} = 1$ if $(i, j) \in \mathcal{E}$, where $i \neq j$. The adjacency and target matrices corresponding to the example in Figure 1(A) are

$$\mathcal{A} = \begin{bmatrix} 0 & 1 & 0 & 0 \\ 0 & 0 & 1 & 0 \\ 0 & 0 & 0 & 1 \\ 0 & 0 & 0 & 0 \end{bmatrix}, \quad \mathcal{B} = \begin{bmatrix} 1 & 0 & 0 & 0 \\ 0 & 0 & 0 & 0 \\ 0 & 0 & 0 & 0 \\ 0 & 0 & 0 & 0 \end{bmatrix}.$$

As shown in Figure 1(B), it is also possible to combine the one-vehicle look-ahead topology with a leader-to-all communication, where $\mathcal{V} = \{1, 2, 3, 4\}$, $\mathcal{E} = \{(1, 2), (2, 3), (3, 4)\}$ and $\mathcal{T} = \{1, 2, 3, 4\}$. The adjacency and target matrices of this topology are

$$\mathcal{A} = \begin{bmatrix} 0 & 1 & 0 & 0 \\ 0 & 0 & 1 & 0 \\ 0 & 0 & 0 & 1 \\ 0 & 0 & 0 & 0 \end{bmatrix}, \quad \mathcal{B} = \begin{bmatrix} 1 & 0 & 0 & 0 \\ 0 & 1 & 0 & 0 \\ 0 & 0 & 1 & 0 \\ 0 & 0 & 0 & 1 \end{bmatrix}.$$

The two-vehicles look-ahead topology is shown in Figure 1(C): it is a generalization of the one-vehicle look-ahead topology, in which connections with more neighbors are available. Here, $\mathcal{V} = \{1, 2, 3, 4\}$, $\mathcal{E} = \{(1, 2), (1, 3), (2, 3), (2, 4), (3, 4)\}$ and $\mathcal{T} = \{1, 2\}$. The adjacency and target matrices of this topology are

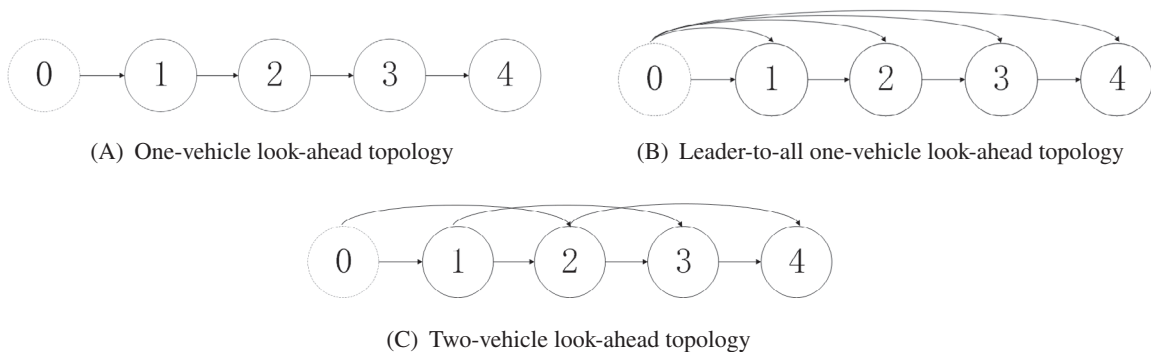


FIGURE 1 Platoon topologies commonly used in cooperative adaptive cruise control

$$A = \begin{bmatrix} 0 & 1 & 1 & 0 \\ 0 & 0 & 1 & 1 \\ 0 & 0 & 0 & 1 \\ 0 & 0 & 0 & 0 \end{bmatrix}, \quad B = \begin{bmatrix} 1 & 0 & 0 & 0 \\ 0 & 1 & 0 & 0 \\ 0 & 0 & 0 & 0 \\ 0 & 0 & 0 & 0 \end{bmatrix}.$$

In the following section, we will see how to create adaptation laws for the controllers in Section 2, and for the topologies presented in Figure 1.

4 | ADAPTIVE PROTOCOL

As mentioned in Section 2, because of the unknown parameters of vehicle i , it is necessary to propose a new adaptive control law to deal with this condition. This problem is solved hereafter along four synchronization cases, represented in Figure 2: synchronization to leader (Section 4.1), synchronization to one vehicle ahead (Section 4.2), synchronization to one vehicle ahead and leader (Section 4.3), synchronization to two vehicles ahead (Section 4.4).

4.1 | Case 1: Synchronization to leader

The first case is synchronizing the target vehicle to the reference model. The network under the consideration is presented in Figure 2(A). In line with the problem of Section 2, to deal with the unknown parameters, we come up with a control law as below

$$u_1 = l_1 \frac{1}{s + \lambda_0} u_1 + f_1 \frac{1}{s + \lambda_0} y_1 + g_1 y_1 + c_1 r + u_{1aux}, \tag{20}$$

where the parameter vector l_1, f_1, g_1, c_1 are the estimates of $l_1^*, f_1^*, g_1^*, c_1^*$, respectively, and u_{1aux} is an extra control action that will be defined later.

The controller (20) can be written in a state-space form by using auxiliary filters

$$\begin{aligned} \dot{\omega}_{u1} &= -\lambda_0 \omega_{u1} + u_1, \\ \dot{\omega}_{y1} &= -\lambda_0 \omega_{y1} + y_1, \\ \dot{\phi}_1 &= -p_0 \phi_1 + \omega_1, \\ \dot{\theta}_1 &= -\Gamma_1 e_{10} \phi_1. \end{aligned} \tag{21}$$

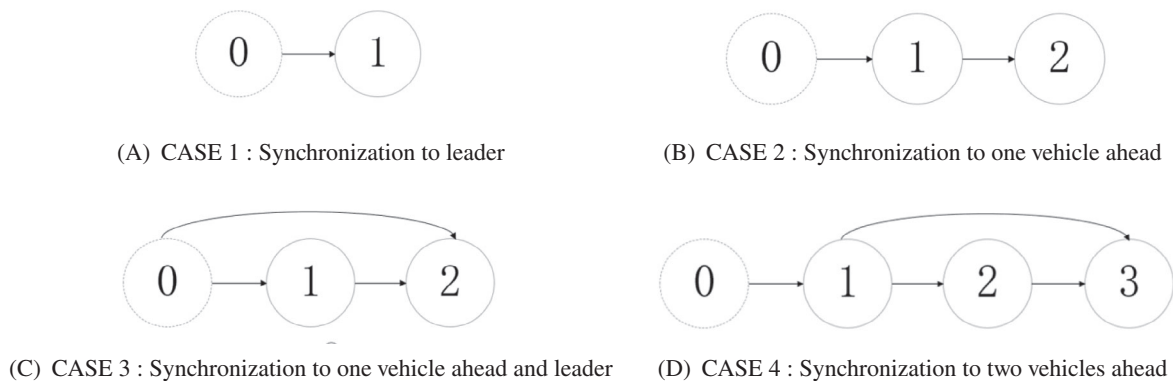


FIGURE 2 Four common platoon synchronization cases

with $\omega_1 = (\omega_{u1} \ \omega_{y1} \ y_1 \ r)^T$, $\theta_1 = (l_1 \ f_1 \ g_1 \ c_1)^T$, $e_{10} = y_1 - y_0$, and $p_0 > 0$ is a real number to be designed, and Γ_1 is a positive symmetric matrix to be designed. The third filter is due to the fact that the relative degree of the system is 2 ($n^* = 2$). Thus, the control law is given by

$$u_1 = \theta_1^T \omega_1 + \dot{\theta}_1^T \phi_1 \quad (22)$$

where we see that $u_{1\text{aux}}$ in (20) is $\dot{\theta}_1^T \phi_1$.

The adaptive gain is defined as

$$\Gamma_1 = \text{diag}\{\Gamma_l, \Gamma_f, \Gamma_g, \Gamma_c\}, \quad (23)$$

where $\Gamma_l, \Gamma_f, \Gamma_g, \Gamma_c$ are the positive real numbers to be designed. The following result holds.

Theorem 1. Consider the reference model dynamics (3), the unknown vehicle dynamics (1) with $i = 1$, the controller (22), and the adaptive laws (21). Then, all the closed-loop signals are bounded and the error $e_{10} \rightarrow 0$ for $t \rightarrow \infty$.

Proof. Since this proof is based on a well-known result from Reference 33, we just recall the main steps, in order to clarify how the adaptive laws (21) are obtained. Using canonical state-space representation to describe the dynamics of reference model 0 and vehicle 1, we have

$$\begin{aligned} \dot{x}_0 &= A_0 x_0 + B_0 r, \\ y_0 &= C_0 x_0. \end{aligned} \quad (24)$$

$$\begin{aligned} \dot{x}_1 &= A_1 x_1 + B_1 u_1, \\ y_1 &= C_1 x_1. \end{aligned} \quad (25)$$

where $A_0, B_0, C_0, A_1, B_1, C_1$ are matrices with proper dimensions. Define the state-space representation of vehicle 1 in a closed-loop form

$$\begin{aligned} \dot{\bar{x}}_1 &= \bar{A}_1 \bar{x}_1 + \bar{B}_1 c_1^* r + \bar{B}_1 (u_1 - \theta_1^{*T} \omega_1), \\ \bar{y}_1 &= \bar{C}_1 \bar{x}_1. \end{aligned} \quad (26)$$

where

$$\bar{x}_1 = \begin{bmatrix} x_1^T & \omega_{u_1} & \omega_{y_1} \end{bmatrix}^T, \quad \bar{A}_1 = \begin{bmatrix} A_1 + B_1 g_1^* C_1^T & B_1 l_1^* & B_1 f_1^* \\ g_1^* C_1^T & -\lambda_0 + l_1^* & f_1^* \\ C_1^T & 0 & -\lambda_0 \end{bmatrix}, \quad \bar{B}_1 = \begin{bmatrix} B_1 \\ 1 \\ 0 \end{bmatrix}, \quad \bar{C}_1 = \begin{bmatrix} C_1 & 0 & 0 \end{bmatrix}.$$

Note that $\bar{y}_1 = y_1$.

When $\bar{C}_1 (sI - \bar{A}_1)^{-1} \bar{B}_1 c_1^* = C_0 (sI - A_0)^{-1} B_0$, vehicle 1 can be matched to vehicle 0. Therefore, the state-space representation of vehicle 1 in a closed-loop form can be written as

$$\begin{aligned} \dot{\bar{x}}_1 &= A_0 \bar{x}_1 + B_0 r + B_0 \rho_1^* (u_1 - \theta_1^{*T} \omega_1), \\ y_1 &= C_0 \bar{x}_1. \end{aligned} \quad (28)$$

where $\rho_1^* = \frac{1}{c_1^*}$.

Define the state tracking error $\tilde{x}_{10} = \bar{x}_1 - x_0$ and the output error $e_{10} = y_1 - y_0$. Then we have

$$\begin{aligned} \dot{\tilde{x}}_{10} &= A_0 \tilde{x}_{10} + B_0 \rho_1^* (u_1 - \theta_1^{*T} \omega_1), \\ e_{10} &= C_0 \tilde{x}_{10}. \end{aligned} \quad (29)$$

Using the identity $(s + p_0)(s + p_0)^{-1} = 1$, we can rewrite (29) as

$$\begin{aligned} \dot{\tilde{x}}_{10} &= A_0 \tilde{x}_{10} + B_0 (s + p_0) \rho_1^* (u_f - \theta_1^{*T} \phi_1), \\ e_{10} &= C_0 \tilde{x}_{10}. \end{aligned} \quad (30)$$

with $u_f = \frac{1}{s+p_0}u_1$. Then, we can choose

$$u_f = \theta_1^T \phi_1, \tag{31}$$

so (30) can be shown as

$$\begin{aligned} \dot{\tilde{x}}_{10} &= A_0\tilde{x}_{10} + B_0(s + p_0)\rho_1^*\tilde{\theta}_1^T \phi_1, \\ e_{10} &= C_0\tilde{x}_{10}. \end{aligned} \tag{32}$$

where $\tilde{\theta}_1 = \theta_1 - \theta_1^*$. The estimation error can be transformed into the desired form by using the transformation

$$\begin{aligned} \bar{e}_1 &= \tilde{x}_{10} - B_0\rho_1^*\tilde{\theta}_1 \phi_1, \\ \dot{\bar{e}}_1 &= A_0\bar{e}_1 + B_k\rho_1^*\tilde{\theta}^T \phi, \\ e_{10} &= C_0\bar{e}_1. \end{aligned} \tag{33}$$

where $B_k = A_0B_0 + B_0p_0$, and $C_0B_0 = 0$ since $n = 2$.

To show the asymptotic convergence of the error between the vehicle 1 and the leader analytically, construct the following Lyapunov function

$$V_1(\tilde{\theta}_1, \bar{e}_1) = \frac{\bar{e}_1^T P \bar{e}_1}{2} + \frac{\tilde{\theta}_1^T \Gamma_1^{-1} \tilde{\theta}_1}{2} |\rho_1^*|, \tag{34}$$

where $P = P^T > 0$ satisfies

$$PA_0 + A_0^T P = -qq^T - \nu L, \quad PB_k = C_0. \tag{35}$$

with $L = L^T > 0$, and $\nu > 0$. So the time derivative of V_1 is

$$\dot{V}_1 = -\frac{\bar{e}_1^T qq^T \bar{e}_1}{2} - \frac{\nu \bar{e}_1^T L \bar{e}_1}{2} + PB_k \bar{e}_1 \rho_1^* \tilde{\theta}_1^T \phi_1 + \tilde{\theta}_1^T \Gamma_1^{-1} \dot{\tilde{\theta}}_1 |\rho_1^*|, \tag{36}$$

since $PB_k \bar{e}_1 = C_0 \bar{e}_1 = e_{10}$ and $\rho_1^* = |\rho_1^*|$, we can make $\dot{V}_1 \leq 0$ by choosing

$$\dot{\tilde{\theta}}_1 = -\Gamma_1 e_{10} \phi_1, \tag{37}$$

which leads to

$$\dot{V}_1 = -\frac{\bar{e}_1^T qq^T \bar{e}_1}{2} - \frac{\nu \bar{e}_1^T L \bar{e}_1}{2} \leq 0. \tag{38}$$

We can obtain that V_1 has a finite limit by (38), so $\bar{e}_{10}, \tilde{\theta}_1, \tilde{x}_{10} \in \mathcal{L}_\infty$. Because $\tilde{x}_{10} = \bar{x}_1 - \bar{x}_0 \in \mathcal{L}_\infty$ and $\bar{x}_0 \in \mathcal{L}_\infty$, so $\bar{x}_1 \in \mathcal{L}_\infty$. This implies that $x_1, y_1, \omega_1, \omega_2 \in \mathcal{L}_\infty$. Since $y_1, y_0 \in \mathcal{L}_\infty$, we have $\phi_1 \in \mathcal{L}_\infty$. From $u_1 = \theta_1^T \omega_1 + \tilde{\theta}_1^T \phi_1$ and $\theta_1, \omega_1, \phi_1 \in \mathcal{L}_\infty$, we have $u_1 \in \mathcal{L}_\infty$. Therefore, all signals in the closed-loop system are bounded. From (38) we can establish that \dot{V}_1 has a bounded integral, so we have $\tilde{x}_{10}, e_{10} \in \mathcal{L}_2$. Using $\theta_1, \omega_1, \tilde{x}_{10} \in \mathcal{L}_\infty$, in (29), we have $e_{10}, \dot{\tilde{x}}_{10} \in \mathcal{L}_\infty$. This implies $e_{10} \rightarrow 0$ for $t \rightarrow \infty$. ■

4.2 | Case 2: Synchronization to one vehicle ahead

As shown in Figure 2(B), case 2 deals with synchronization of vehicle 2 to one vehicle ahead (vehicle 1), without information from reference dynamics. In this case, the control law (22) and the matching condition have two problems. The

first problem is that we do not know the gains l_1^*, f_1^*, g_1^* , and c_1^* . The second problem is that, the control law (22) would be implementable only if vehicle connected to the reference model vehicle 0, and with access to r .

Motivated by the control (9), then we come up the following controller

$$u_2 = l_{21} \frac{1}{s + \lambda_0} u_1 + f_{21} \frac{1}{s + \lambda_0} y_1 + g_{21} y_1 + c_{21} u_1 + l_2 \frac{1}{s + \lambda_0} (u_2 - u_1) + f_2 \frac{1}{s + \lambda_0} (y_2 - y_1) + g_2 (y_2 - y_1) + u_{2\text{aux}}, \quad (39)$$

where the controller parameter vector $l_{21}, l_2, f_{21}, f_2, g_{21}, g_1$, and c_{21} are the estimates for $l_{21}^*, l_2^*, f_{21}^*, f_2^*, g_{21}^*, g_1^*$, and c_{21}^* , respectively, and $u_{2\text{aux}}$ is an auxiliary term to be defined.

These estimates are updated via the following adaptive laws

$$\begin{aligned} \dot{\omega}_{u_1} &= -\lambda_0 \omega_{u_1} + u_1, & \dot{\omega}_{u_{21}} &= -\lambda_0 \omega_{u_{21}} + (u_2 - u_1), \\ \dot{\omega}_{y_1} &= -\lambda_0 \omega_{y_1} + y_1, & \dot{\omega}_{y_{21}} &= -\lambda_0 \omega_{y_{21}} + (y_2 - y_1), \\ \dot{\phi}_2 &= -p_0 \phi_2 + \omega_2, & \dot{\theta}_2 &= -\Gamma_2 e_{21} \phi_2, \end{aligned} \quad (40)$$

in which $e_{21} = y_2 - y_1$ and

$$\begin{aligned} \omega_2 &= [\omega_{u_1} \quad \omega_{y_1} \quad y_1 \quad u_1 \quad \omega_{u_{21}} \omega_{y_{21}} \quad e_{21}]^T, \\ \theta_2 &= [l_{21} \quad f_{21} \quad g_{21} \quad c_{21} \quad l_2 \quad f_2 \quad g_2]^T, \\ \Gamma_2 &= \text{diag}\{\Gamma_l, \Gamma_f, \Gamma_g, \Gamma_c, \Gamma_l, \Gamma_f, \Gamma_g\}. \end{aligned} \quad (41)$$

where $\Gamma_l, \Gamma_f, \Gamma_g, \Gamma_c$ are the positive real numbers to be designed.

The control input can be given as

$$u_2 = \theta_2^T \omega_2 + \dot{\theta}_2^T \phi_2, \quad (42)$$

where we see that $u_{2\text{aux}}$ in (39) is $\dot{\theta}_2^T \phi_2$. The following result holds.

Theorem 2. Consider the unknown vehicle ahead dynamics (1) with subscript $i = 1$, the unknown follower dynamics (2) with subscript $j = 2$, adaptive laws (40) and controllers (42). Then, all closed-loop signals will be bounded and the error $e_{21} \rightarrow 0$ for $t \rightarrow \infty$.

Proof. First let us use the state-space representation to write the vehicle 2 dynamics

$$\begin{aligned} \dot{x}_2 &= A_2 x_2 + B_2 u_2, \\ y_2 &= C_2 x_2. \end{aligned} \quad (43)$$

The closed-loop form allows us to write

$$\begin{aligned} \dot{\bar{x}}_2 &= \bar{A}_2 \bar{x}_2 + \bar{B}_2 c_{21}^* \bar{u}_2 + \bar{B}_2 (u_2 - \theta_2^{*T} \omega_2), \\ \bar{y}_2 &= \bar{C}_2 \bar{x}_2. \end{aligned} \quad (44)$$

where

$$\bar{x}_2 = \begin{bmatrix} x_2^T \\ \omega_{u_1} \\ \omega_{y_1} \\ \omega_{u_{21}} \\ \omega_{y_{21}} \end{bmatrix}, \bar{u}_2 = \begin{bmatrix} u_1 \\ y_1 \end{bmatrix}, \bar{A}_2 = \begin{bmatrix} A_2 + B_2 g_2^* C_2^T & B_2 l_{21}^* & B_2 f_{21}^* & B_2 l_2^* & B_2 f_2^* \\ 0 & -\lambda_0 & 0 & 0 & 0 \\ C_2^T & 0 & -\lambda_0 & 0 & 0 \\ g_2^* C_2^T & l_{21}^* & f_{21}^* & -\lambda_0 + l_2^* & f_2^* \\ C_2^T & 0 & 0 & 0 & -\lambda_0 \end{bmatrix}, \bar{B}_2 = \begin{bmatrix} B_2 & \frac{B_2 (g_{21}^* - g_2^*)}{c_{21}^*} \\ \frac{1}{c_{21}^*} & 0 \\ 0 & \frac{2}{c_{21}^*} \\ \left(1 - \frac{1}{c_{21}^*}\right) & \frac{(g_{21}^* - g_2^*)}{c_{21}^*} \\ 0 & \frac{1}{c_{21}^*} \end{bmatrix}, \bar{C}_2 = \begin{bmatrix} C_2^T \\ 0 \\ 0 \\ 0 \\ 0 \end{bmatrix}^T.$$

Note that $\bar{y}_2 = y_2$. From (14), we already know that vehicle 2 can match vehicle 1, which results in $\bar{C}_2(sI - \bar{A}_2)^{-1}\bar{B}_2c_{21}^* = \bar{C}_1(sI - \bar{A}_1)^{-1}\bar{B}_1c_{11}^*$. Therefore, vehicle 2 can match the reference model, giving $\bar{C}_2(sI - \bar{A}_2)^{-1}\bar{B}_2c_{21}^* = C_0(sI - A_0)^{-1}B_0$. We can take a nonminimal state-space representation of vehicle 2:

$$\begin{aligned}\dot{\bar{x}}_2 &= A_0\bar{x}_2 + B_0r + B_0\rho_2^*(u_2 - \theta_2^{*T}\omega_2), \\ y_2 &= C_0\bar{x}_2.\end{aligned}\tag{46}$$

where $\rho_2^* = \frac{1}{c_{21}^*}$. Then, define the state tracking error $\tilde{x}_{21} = \bar{x}_2 - \bar{x}_1$, and the output error $e_{21} = y_2 - y_1$. Using the identity $(s + p_0)(s + p_0)^{-1} = 1$ for some $p_0 > 0$, The estimation error can be transformed into the desired form by using the transformation

$$\begin{aligned}\bar{e}_2 &= \bar{x}_{21} - B_0\rho_2^*\tilde{\theta}_2^T\phi_2, \\ \dot{\bar{e}}_2 &= A_0\bar{e}_2 + B_{k_2}\rho_2^*\tilde{\theta}^T\phi, \\ e_{21} &= C_0\bar{e}_2.\end{aligned}\tag{47}$$

where $B_{k_2} = A_0B_0 + B_0p_0$, and we have $u_2 = \theta_2^T\omega_2 + \dot{\theta}_2^T\phi_2$, where $\tilde{\theta}_2^* = \theta_2 - \theta_2^*$. To show the asymptotic converge of the synchronization error analytically, the Lyapunov-based approach will be used, construct the following Lyapunov function

$$V_2(\tilde{\theta}_2, \bar{e}_2) = \frac{\bar{e}_2^T P \bar{e}_2}{2} + \frac{\tilde{\theta}_2^T \Gamma_2^{-1} \tilde{\theta}_2}{2} |\rho_2^*|,\tag{48}$$

where $\Gamma_2 = \Gamma_2^T > 0$ and the $P = P^T > 0$ satisfies

$$PA_0 + A_0^T P = -qq^T - vL, \quad PB_{k_2} = C_0.\tag{49}$$

With $L > 0$, The time derivative becomes

$$\dot{V}_2 = -\frac{\bar{e}_2^T qq^T \bar{e}_2}{2} - \frac{v}{2} \bar{e}_2^T L \bar{e}_2 + PB_0 \bar{e}_2 \rho_2^* \tilde{\theta}_2^T \phi_2 + \tilde{\theta}_2^T \Gamma_2^{-1} \dot{\tilde{\theta}}_2 |\rho_2^*|,\tag{50}$$

since $PB_0 \bar{e}_2 = \bar{C}_0 \bar{e}_2 = e_{21}$ and $\rho_2^* = |\rho_2^*|$, we can delete the indefinite term by choosing

$$\dot{\tilde{\theta}}_2 = -\Gamma_2 e_{21} \phi_2,\tag{51}$$

which leads to

$$\dot{V}_2 = -\frac{\bar{e}_2^T qq^T \bar{e}_2}{2} - \frac{v}{2} \bar{e}_2^T L \bar{e}_2 \leq 0.\tag{52}$$

From (52), it can be obtained that V_2 has a finite limit, so $\bar{e}_2, \tilde{x}_{21}, \tilde{\theta}_2 \in \mathcal{L}_\infty$. Because $\tilde{x}_{21} = \bar{x}_2 - \bar{x}_1 \in \mathcal{L}_\infty$ and $\bar{x}_1 \in \mathcal{L}_\infty$, so $\bar{x}_2 \in \mathcal{L}_\infty$. This implies $x_2, y_2, \omega_{u1}, \omega_{y1}, \omega_{u21}, \omega_{y21} \in \mathcal{L}_\infty$. Since $y_2, y_1 \in \mathcal{L}_\infty$, we have $\phi_2 \in \mathcal{L}_\infty$. From $u_2 = \theta_2^T \omega_2 + \dot{\theta}_2^T \phi_2$ and $\theta_2, \omega_2, \phi_2 \in \mathcal{L}_\infty$, we have $u_2 \in \mathcal{L}_\infty$. Therefore, all signals in the closed-loop system are bounded. From (52) we can establish that \dot{V}_2 has a bounded integral, so we have $\tilde{x}_{21}, e_{21} \in \mathcal{L}_2$. Using $\theta_2, \omega_2, \tilde{x}_{21} \in \mathcal{L}_\infty$, in (40), we can get $e_{21}, \dot{\tilde{x}}_{21} \in \mathcal{L}_\infty$. This implies $e_{21} \rightarrow 0$ for $t \rightarrow \infty$, which concludes the proof. ■

4.3 | Case 3: Synchronization to one vehicle ahead and leader

In line with Figure 2(C), this case deals with the synchronization problem of vehicle 2 to vehicle 1 and leader. This case is especially useful in leader-to-all topologies where in addition to intervehicle communication, the leader can send information to all vehicles in the platoon. It is not a surprise that this case can be solved using a combination of cases 1 and 2. Therefore, only address the main steps.

By following an approach similar to that taken in the previous case, the synchronization of vehicle 2 to vehicle 1 is possible via the controller.

$$u_2 = l_{21} \frac{1}{s + \lambda_0} u_1 + f_{21} \frac{1}{s + \lambda_0} y_1 + g_{21} y_1 + c_{21} u_1 + l_2 \frac{1}{s + \lambda_0} (u_2 - u_1) + f_2 \frac{1}{s + \lambda_0} (y_2 - y_1) + g_2 (y_2 - y_1) + u_{21\text{aux}}, \quad (53)$$

and the synchronization of vehicle 2 to leader is possible via the controller

$$u_2 = l_2 \frac{1}{s + \lambda_0} u_2 + f_2 \frac{1}{s + \lambda_0} y_2 + g_2 y_2 + c_2 r + u_{20\text{aux}}, \quad (54)$$

where $u_{21} = u_2 - u_1$, and the output error $e_{21} = y_2 - y_1$, by combining this, the controller can be obtained

$$u_2 = l_{21} \frac{1}{2(s + \lambda_0)} u_1 + f_{21} \frac{1}{2(s + \lambda_0)} y_1 + \frac{g_{21}}{2} y_1 + \frac{c_{21}}{2} u_1 + l_2 \frac{1}{2(s + \lambda_0)} (u_{21} + u_2) + f_2 \frac{1}{2(s + \lambda_0)} (e_{21} + y_2) + \frac{g_2}{2} (e_{21} + y_2) + \frac{c_2}{2} r + \frac{u_{2\text{aux}}}{2}, \quad (55)$$

where the controller parameter vector $l_{21}, l_2, f_{21}, f_2, g_{21}, g_1$, and c_{21} are the estimates of $l_{21}^*, l_2^*, f_{21}^*, f_2^*, g_{21}^*, g_1^*$, and c_{21}^* , respectively, and $u_{2\text{aux}} = u_{21\text{aux}} + u_{20\text{aux}}$ is an extra control action that will be defined later. These estimate parameter are updated via the following adaptive laws

$$\begin{aligned} \dot{\omega}_{u_1} &= -\lambda_0 \omega_{u_1} + u_1, & \dot{\omega}_{y_1} &= -\lambda_0 \omega_{y_1} + y_1, \\ \dot{\omega}_{u_2} &= -\lambda_0 \omega_{u_2} + u_2, & \dot{\omega}_{y_2} &= -\lambda_0 \omega_{y_2} + y_2, \\ \dot{\omega}_{u_{21}} &= -\lambda_0 \omega_{u_{21}} + u_{21}, & \dot{\omega}_{y_{21}} &= -\lambda_0 \omega_{y_{21}} + e_{21}, \\ \dot{\phi}_2 &= -p_0 \phi_2 + \omega_2, & \dot{\theta}_2 &= -\Gamma_2 e_{210} \phi_2, \end{aligned} \quad (56)$$

in which $e_{210} = (y_2 - y_1) + (y_2 - y_0)$, and

$$\omega_2 = \begin{bmatrix} \omega_{u_1} & \omega_{y_1} & y_1 & u_1 & (\omega_{u_{21}} + \omega_{u_2}) & (\omega_{y_{21}} + \omega_{y_2}) & (e_{21} + y_2) & r \end{bmatrix},$$

$$\theta_2 = \begin{bmatrix} l_{21} & f_{21} & g_{21} & c_{21} & l_2 & f_2 & g_2 & c_2 \end{bmatrix}^T$$

$$\Gamma_2 = \text{diag}\{\Gamma_l, \Gamma_f, \Gamma_g, \Gamma_c, \Gamma_l, \Gamma_f, \Gamma_g, \Gamma_c\},$$

where $\Gamma_l, \Gamma_f, \Gamma_g, \Gamma_c$ are the positive real numbers to be designed. the control input can be given as

$$u_2 = \frac{\theta_2^T \omega_2}{2} + \frac{\tilde{\theta}_2^T \phi_2}{2}, \quad (57)$$

where $u_{2\text{aux}} = \tilde{\theta}_2^T \phi_2$. The following result holds.

Theorem 3. Consider the leader dynamics (3), the unknown vehicle ahead dynamics (1) with subscript $i = 1$, the unknown follower dynamics (2) with subscript $j = 2$, the controllers (57), and the adaptive laws (56). Then, all closed-loop signals will be bounded and the error $e_{210} \rightarrow 0$ for $t \rightarrow \infty$ (i.e., the vehicle 2 can synchronize to vehicle 1 and leader).

Proof. The proof, not shown to avoid repetitions, follows similar steps as the previous cases and makes use of the Lyapunov function

$$V_2(\tilde{\theta}_2, \bar{e}_{210}) = \frac{\bar{e}_{210}^T P \bar{e}_{210}}{2} + \frac{\tilde{\theta}_2^T \Gamma_2^{-1} \tilde{\theta}_2}{2} |\rho_2^*|. \quad (58)$$

4.4 | Case 4: Synchronization to two vehicles ahead

In this case, we will discuss how vehicle 3 can synchronize to two vehicles ahead, as shown in Figure 2(D). Note that $\tau_1, \tau_2,$ and τ_3 are possibly different. There exist a directed connection from vehicle 1 to vehicle 3 and a directed connection from vehicle 2 to vehicle 3. So, vehicle 3 can observe measurement from vehicle 1 to vehicle 2, respectively. By following an approach similar to that taken in the previous cases, the synchronization of vehicle 3 to vehicle 1 is possible via the controller.

$$\begin{aligned}
 u_3 = & l_{31} \frac{1}{(s+1)} u_1 + f_{31} \frac{1}{(s+1)} y_1 + g_{31} y_1 + c_{31} u_1 \\
 & + l_3 \frac{1}{(s+1)} u_{31} + f_3 \frac{1}{(s+1)} e_{31} + g_3 e_{31} + u_{31aux},
 \end{aligned} \tag{59}$$

and the synchronization of vehicle 3 to vehicle 2 is possible via the controller

$$\begin{aligned}
 u_3 = & l_{32} \frac{1}{(s+1)} u_2 + f_{32} \frac{1}{(s+1)} y_2 + g_{32} y_2 + c_{32} u_2 \\
 & + l_3 \frac{1}{(s+1)} u_{32} + f_3 \frac{1}{(s+1)} e_{32} + g_3 e_{32} + u_{32aux},
 \end{aligned} \tag{60}$$

where $u_{31} = u_3 - u_1$ and $u_{32} = u_3 - u_2$, and the output error $e_{31} = y_3 - y_1, e_{32} = y_3 - y_2$. By combining the two controllers, we obtain

$$\begin{aligned}
 u_3 = & l_{31} \frac{1}{2(s+1)} u_1 + f_{31} \frac{1}{2(s+1)} y_1 + \frac{g_{31} y_1}{2} + \frac{c_{31} u_1}{2} + l_{32} \frac{1}{2(s+1)} u_2 + f_{32} \frac{1}{2(s+1)} y_2 + \frac{g_{32} y_2}{2} \\
 & + \frac{c_{32} u_2}{2} + l_3 \frac{1}{2(s+1)} u_{321} + f_3 \frac{1}{2(s+1)} e_{321} + \frac{g_3 e_{321}}{2} + \frac{u_{3aux}}{2},
 \end{aligned} \tag{61}$$

where

$$\begin{aligned}
 u_{321} = & u_{31} + u_{32}, & e_{321} = & e_{31} + e_{32}, \\
 \theta_3 = & \theta_{31} + \theta_{32}, & \omega_3 = & \omega_{31} + \omega_{32},
 \end{aligned} \tag{62}$$

and $u_{3aux} = u_{31aux} + u_{32aux}$ is an auxiliary input to be designed.

The controller parameter vector $l_{31}, l_{21}, l_2, f_{31}, f_{21}, f_2, g_{31}, g_{21}, g_1,$ and c_{21}, c_{31} are the estimates for $l_{31}^*, l_{21}^*, l_2^*, f_{31}^*, f_{21}^*, f_2^*, g_{31}^*, g_{21}^*, g_1^*,$ and $c_{21}^*, c_{31}^*,$ respectively. These estimate parameter are updated via the following adaptive laws

$$\begin{aligned}
 \dot{\omega}_{u_1} = & -\lambda_0 \omega_{u_1} + u_1, & \dot{\omega}_{y_1} = & -\lambda_0 \omega_{y_1} + y_1, \\
 \dot{\omega}_{u_2} = & -\lambda_0 \omega_{u_2} + u_2, & \dot{\omega}_{y_2} = & -\lambda_0 \omega_{y_2} + y_2, \\
 \dot{\omega}_{u_{321}} = & -\lambda_0 \omega_{u_{321}} + u_{321}, & \dot{\omega}_{e_{321}} = & -\lambda_0 \omega_{e_{321}} + e_{321}, \\
 \dot{\theta}_3 = & -\Gamma_3 e_{321} \phi_3, & \dot{\phi}_3 = & -p_0 \phi_3 + \omega_3,
 \end{aligned} \tag{63}$$

where

$$\begin{aligned}
 \omega_3 = & \left[\omega_{u_1} \quad \omega_{y_1} \quad y_1 \quad u_1 \quad \omega_{u_2} \quad \omega_{y_2} \quad y_2 \quad u_2 \quad \omega_{u_{321}} \quad \omega_{e_{321}} \quad e_{321} \right]^T, \\
 \theta_3 = & \left[l_{31} \quad f_{31} \quad g_{31} \quad c_{31} \quad l_{32} \quad f_{32} \quad g_{32} \quad c_{32} \quad l_3 \quad f_3 \quad g_3 \right]^T, \\
 \Gamma_3 = & \text{diag}\{\Gamma_l, \Gamma_f, \Gamma_g, \Gamma_c, \Gamma_l, \Gamma_f, \Gamma_g, \Gamma_l, \Gamma_l, \Gamma_f, \Gamma_g\},
 \end{aligned}$$

and $\Gamma_l, \Gamma_f, \Gamma_g, \Gamma_c$ are the positive real numbers to be designed. the control input can be given as

$$u_3 = \frac{\theta_3^T \omega_3}{2} + \frac{\dot{\theta}_3^T \phi_3}{2}. \tag{64}$$

where $u_{3\text{aux}} = \dot{\theta}_3^T \phi_3$. The following result holds.

Theorem 4. Consider the unknown vehicle dynamics (1) with subscript $i = 1$, the unknown vehicle dynamics (2) with subscript $j = 2$, and the unknown vehicle dynamics (2) with subscript $j = 3$, the controllers (64), and the adaptive laws (63). Then, all the closed-loop signals will be bounded and the error $e_{321} \rightarrow 0$ for $t \rightarrow \infty$ (i.e., the vehicle 3 can synchronize to vehicles 1 and 2).

Proof. The proof, not shown to avoid repetitions, follows similar steps as the previous cases and makes use of the Lyapunov function

$$V_3(\tilde{\theta}_3, \bar{e}_{321}) = \frac{\bar{e}_{321}^T P \bar{e}_{321}}{2} + \frac{\tilde{\theta}_3^T \Gamma_3^{-1} \tilde{\theta}_3}{2} |\rho_3^*|. \quad (65)$$

5 | SIMULATIONS

This section shows the simulation results of three topologies in Figure 1, in this simulation, five vehicles (one leader vehicle and four following vehicles) are simulated. The parameters of leader vehicle and of the other vehicles are given as $a_0 = 0.0625$, $a_1 = 0.4$, $k_0 = 0.0625$, $k_1 = 0.5$, $k_2 = 0.6$, $k_3 = 0.7$, $k_4 = 0.8$. The control parameters are chosen as $\Gamma_l = 0.1$, $\Gamma_f = 2 \cdot 10^{-6}$, $\Gamma_g = 3 \cdot 10^{-5}$, $p_0 = 1 \cdot 10^{-6}$, and the desired distance r_{ji} between each vehicle is 5 m.

5.1 | Simulation results of the topology 1

As shown in Figure 1(A), the first simulation considers a classic one-vehicle look-ahead topology, where each vehicle can observe acceleration information of the preceding vehicle. And Figure 3 shows the acceleration response of each vehicle. The velocity response and the relative distances of each vehicles with the leader vehicle are given in Figures 4 and 5, respectively. It is clear that all the vehicles will synchronize to the leader vehicle and keep the desired distances with each other.

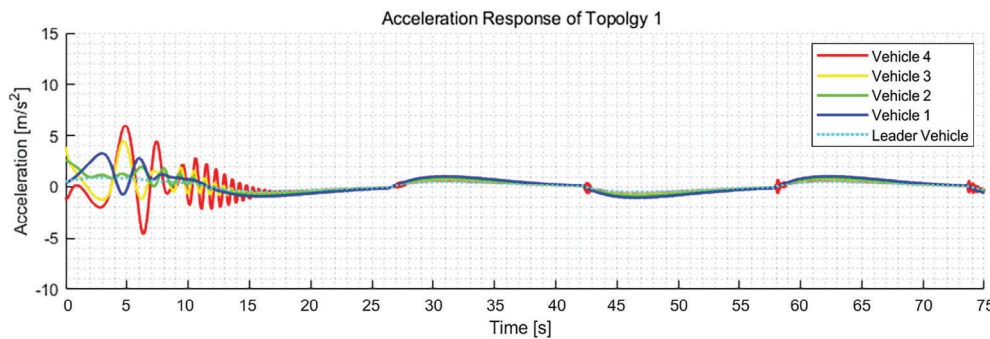


FIGURE 3 Acceleration response of topology 1

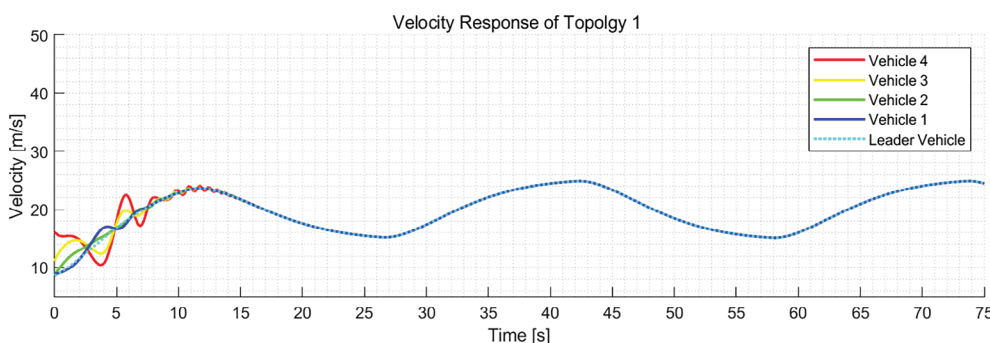


FIGURE 4 Velocity response of topology 1

FIGURE 5 Relative distances with leader vehicle of topology 1

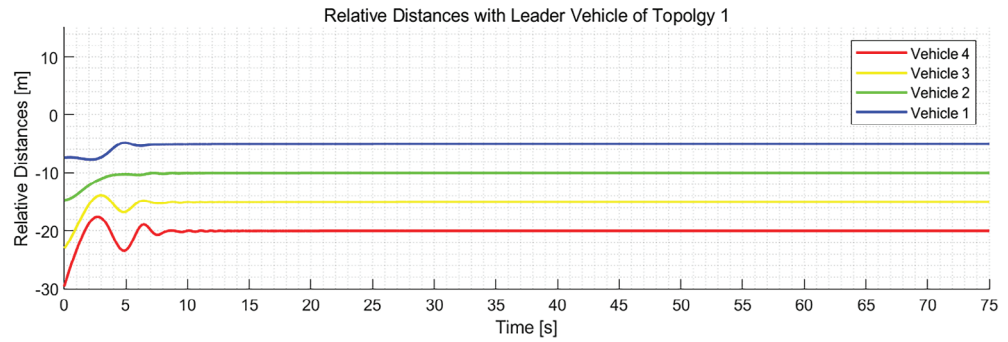


FIGURE 6 Acceleration response of topology 2

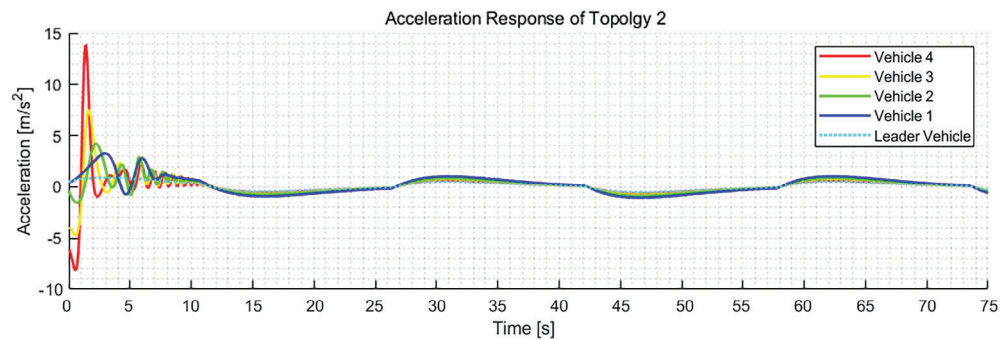
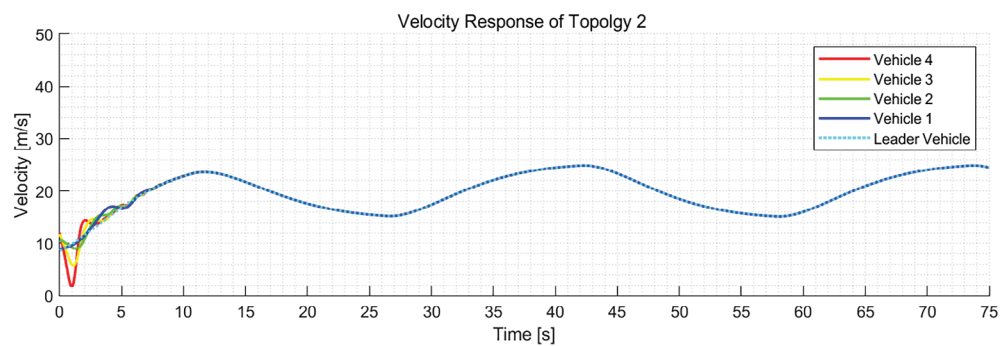


FIGURE 7 Velocity response of topology 2



5.2 | Simulation results of the topology 2

The leader-to-all one-vehicle look-ahead topology is simulated in this part, as described in Figure 1(B), each vehicles can get acceleration information from both the preceding vehicle and the leader. The acceleration response and the velocity response of each vehicle is shown in Figures 6 and 7, respectively. Figure 8 shows the required relative distances is maintained. With respect to topology 1, the response of topology 2 has a bit larger transient, and this might indicate that information from the leader nonnecessarily might lead to better performance.

5.3 | Simulation results of the topology 3

The results of topology 3 is presented in this part, that is a two-vehicle look-ahead situation. In this topology, each vehicle can communicate with two preceding vehicle. It is clear that the on-board laser cannot be use to get the relative spacing with two vehicles ahead. Therefore, the preceding vehicle must communicate the relative spacing with the second preceding vehicle in order to obtain the relative spacing with two vehicles ahead. The acceleration response and the velocity response of each vehicle are is described in Figures 9 and 10, respectively. Again, we obtain the result that all vehicles can synchronize to the leader vehicle and maintain the relative distances in line with Figure 11.

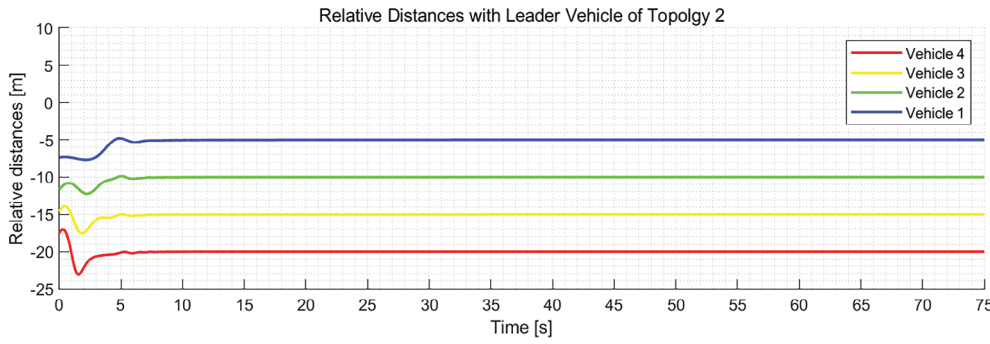


FIGURE 8 Relative distances with leader vehicle of topology 2

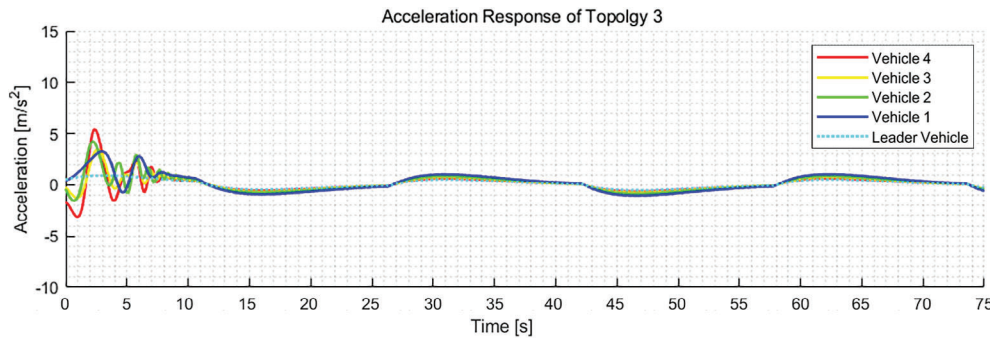


FIGURE 9 Acceleration response of topology 3

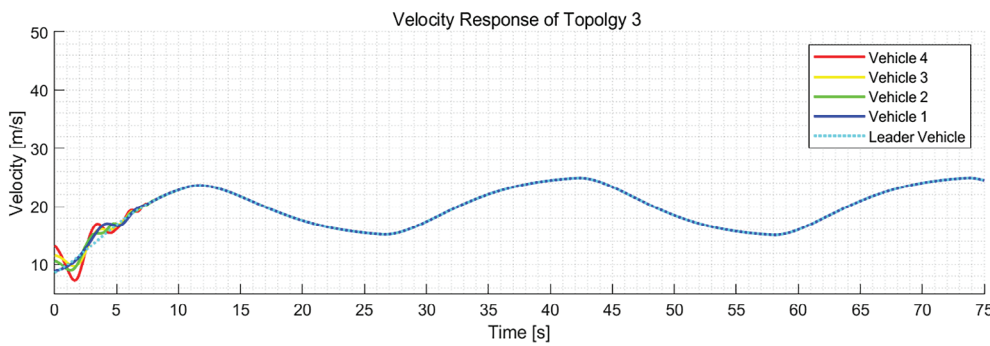


FIGURE 10 Velocity response of topology 3

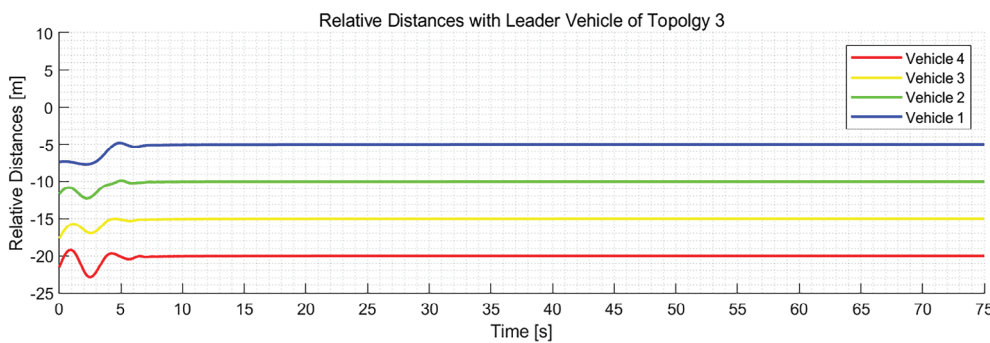


FIGURE 11 Relative distances with leader vehicle of topology 3

6 | CONCLUSIONS

Cooperative driving strategies proposed in literature, also known as CACC strategies, assume that both relative spacing and relative velocity with preceding vehicle are available from on-board sensors (laser or radar). Otherwise, they assume that both velocity states and acceleration from preceding vehicle inputs are communicated. The same sensing and communication also extends to adaptive cooperative driving strategies, where vehicle parametric uncertainty is taken into account. However, in practice on-board sensors can only measure relative spacing with preceding vehicle (since getting

relative velocity requires additional filtering algorithms); also, it is fundamental to reduce the number of variables communicated from preceding vehicle in order to save bandwidth. This work has shown that, after framing the cooperative driving task as a distributed MRAC problem, the platooning task can be achieved in a minimal sensing and communication scenario, that is, by removing relative velocity measurements with preceding vehicle from on-board sensors and removing communication from preceding vehicle of velocity states. The proposed framework was illustrated and shown to be flexible to several standard architectures used in cooperative driving (one-vehicle look-ahead topology, leader-to-all topology, multivehicle look-ahead topology). The simulation results highlight that the two-vehicle look-ahead topology has the best performance, in the sense that it provides a smoother response with less oscillations and smaller peaks. This is consistent with the intuition that better performance can be achieved when more information is available. On the other hand, it is worth mentioning that more communication can also cause interferences and reliability issues.

In practical applications, due to the unreliable wireless of communication conditions and external interference (loss of communication links, addition of new communication links, and so forth), the communication topology between vehicles can be changed.³⁴ So the interesting future research topics are to provide stability on the presence of switching topologies, that can refer to the switching among the standard architectures used in cooperative driving (one-vehicle look-ahead topology, leader-to-all topology, multivehicle look-ahead topology), but also to possible communication losses that might require to use only on-board sensors for implementing the platoon. In addition, is it worth noticing that the proposed approach uses the position as output feedback, which can be obtained from on-board GPS, but still requires some type of communication: it is an interesting future work to remove this communication channel as well. Another relevant future work could be to study input constraints (engine constraints). Some recent advances in this direction are References 22,35.

ACKNOWLEDGMENTS

This work was supported in part by the National Natural Science Foundation of China under Grant 62073074, Grant 61673107, and Grant 62073076; and in part by the Jiangsu Provincial Key Lab of Networked Collective Intelligence under Grant BM2017002.

DATA AVAILABILITY STATEMENT

Data available on request from the authors.

ORCID

Kang Yang  <https://orcid.org/0000-0003-0916-8267>

Wenwu Yu  <https://orcid.org/0000-0002-3194-2258>

REFERENCES

1. Dyda AA, Oskin DA, Longhi S, Monteriù A. An adaptive VSS control for remotely operated vehicles. *Int J Adapt Control Signal Process.* 2017;31(4):507-521.
2. Fisher DL, Lohrenz M, Moore D, Nadler ED, Pollard JK. Humans and intelligent vehicles: the hope, the help, and the harm. *IEEE Trans Intell Veh.* 2016;1(1):56-67.
3. di Bernardo M, Salvi A, Santini S. Distributed consensus strategy for platooning of vehicles in the presence of time-varying heterogeneous communication delays. *IEEE Trans Intell Transp Syst.* 2015;16(1):102-112.
4. Maiti S, Winter S, Kulik L, Sarkar S. The impact of flexible platoon formation operations. *IEEE Trans Intell Veh.* 2020;5(2):229-239.
5. Jin X, Haddad WM, Jiang ZP, Kanellopoulos A, Vamvoudakis KG. An adaptive learning and control architecture for mitigating sensor and actuator attacks in connected autonomous vehicle platoons. *Int J Adapt Control Signal Process.* 2019;33(12):1788-1802.
6. Monteil J, Russo G, Shorten R. On \mathcal{L}_∞ string stability of nonlinear bidirectional asymmetric heterogeneous platoon systems. *Automatica.* 2019;105:198-205.
7. Tóth J, Rödönyi G. String stability preserving adaptive spacing policy for handling saturation in heterogeneous vehicle platoons. *IFAC-PapersOnLine.* 2017;50(1):8525-8530. 20th IFAC World Congress.
8. Wang Y, Gunter G, Nice M, Delle Monache ML, Work D. Online parameter estimation methods for adaptive cruise control systems. *IEEE Trans Intell Veh.* 2020;1. <https://doi.org/10.1109/TIV.2020.3023674>.
9. Naus G, Vugts R, Ploeg J, Molengraaf M, Steinbuch M. String-stable CACC design and experimental validation: a frequency-domain approach. *Veh Technol.* 2010;59:4268-4279.
10. Gunter G, Gloudemans D, Stern RE, et al. Are commercially implemented adaptive cruise control systems string stable? *IEEE Trans Intell Transp Syst.* 2020;1-12. <https://doi.org/10.1109/TITS.2020.3000682>.
11. Turri V, Besselink B, Johansson KH. Cooperative look-ahead control for fuel-efficient and safe heavy-duty vehicle platooning. *IEEE Trans Control Syst Technol.* 2017;25(1):12-28.

12. Milanés V, Shladover SE, Spring J, Nowakowski C, Kawazoe H, Nakamura M. Cooperative adaptive cruise control in real traffic situations. *IEEE Trans Intell Transp Syst.* 2014;15(1):296-305.
13. Giammarino V, Baldi S, Frasca P, Monache MLD. Traffic flow on a ring with a single autonomous vehicle: an interconnected stability perspective. *IEEE Trans Intell Transp Syst.* 2020;1-11. <https://doi.org/10.1109/TITS.2020.2985680>.
14. Li Z, Hu B, Li M, Luo G. String stability analysis for vehicle platooning under unreliable communication links with event-triggered strategy. *IEEE Trans Veh Technol.* 2019;68(3):2152-2164.
15. Kayacan E. Multiobjective H_∞ control for string stability of cooperative adaptive cruise control systems. *IEEE Trans Intell Veh.* 2017;2(1):52-61.
16. Acciani F, Frasca P, Stoorvogel A, Semsar-Kazerouni E, Heijenk G. Cooperative adaptive cruise control over unreliable networks: an observer-based approach to increase robustness to packet loss. Paper presented at: Proceedings of the 2018 European Control Conference (ECC 2018); Limassol, Cyprus, June 12, 2018.;1399-1404.
17. Pirani M, Hashemi E, Khajepour A, et al. Cooperative vehicle speed fault diagnosis and correction. *IEEE Trans Intell Transp Syst.* 2019;20(2):783-789.
18. Ariffin MHM, Rahman MAA, Zamzuri H. Effect of leader information broadcasted throughout vehicle platoon in a constant spacing policy; 2015:132-137.
19. Tao T, Jain V, Baldi S. An adaptive approach to longitudinal platooning with heterogeneous vehicle saturations. *IFAC-PapersOnLine.* 2019;52(3):7-12. 15th IFAC Symposium on Large Scale Complex Systems LSS 2019.
20. Harfouch YA, Shuai Y, Baldi S. Adaptive control of interconnected networked systems with application to heterogeneous platooning Paper presented at: Proceedings of the 2017 13th IEEE International Conference on Control and Automation (ICCA); Ohrid, Macedonia, 2017.
21. Ren W, Beard RW, Atkins EM. Information consensus in multivehicle cooperative control. *IEEE Control Syst Mag.* 2007;27(2):71-82.
22. Baldi S, Liu D, Jain V, Yu W. Establishing platoons of bidirectional cooperative vehicles with engine limits and uncertain dynamics. *IEEE Trans Intell Transp Syst.* 2020;1-13. <https://doi.org/10.1109/TITS.2020.2973799>.
23. Wang C, Nijmeijer H. String stable heterogeneous vehicle platoon using cooperative adaptive cruise control; 2015:1977-1982.
24. Wu Y, Li SE, Cortés J, Poolla K. Distributed sliding mode control for nonlinear heterogeneous platoon systems with positive definite topologies. *IEEE Trans Control Syst Technol.* 2020;28(4):1272-1283.
25. Rödönyi G. Heterogeneous string stability of unidirectionally interconnected MIMO LTI systems. *Automatica.* 2019;103:354-362.
26. Baldi S, Frasca P. Adaptive synchronization of unknown heterogeneous agents: an adaptive virtual model reference approach. *J Franklin Inst.* 2019;356(2):935-955.
27. Roy SB, Bhasin S. Robustness analysis of initial excitation based adaptive control. Paper presented at: Proceedings of the 2019 IEEE 58th Conference on Decision and Control (CDC); 2019.
28. Huang M, Gao W, Jiang ZP. Connected cruise control with delayed feedback and disturbance: an adaptive dynamic programming approach. *International Journal of Adaptive Control and Signal Processing.* 2019;33(2):356-370.
29. Baldi S, Rosa MR, Frasca P, Kosmatopoulos EB. Platooning merging maneuvers in the presence of parametric uncertainty. *IFAC-PapersOnLine.* 2018;51(23):148-153. 7th IFAC Workshop on Distributed Estimation and Control in Networked Systems NECSYS 2018.
30. Muhammad R. Adaptive synchronization for heterogeneous multi-agent systems with switching topologies. *Machines.* 2018;6(1):7.
31. Lu M, Liu L. Cooperative output regulation of linear multi-agent systems by a novel distributed dynamic compensator. *IEEE Trans Automat Contr.* 2017;62(12):6481-6488.
32. Wang W, Wen C, Huang J, Li Z. Hierarchical decomposition based consensus tracking for uncertain interconnected systems via distributed adaptive output feedback control. *IEEE Trans Automat Contr.* 2016;61(7):1938-1945.
33. Ioannou P, Fidan B. *Adaptive Control Tutorial*. Philadelphia: SIAM; 2006.
34. Liu D, Baldi S, Jain V, Yu W, Frasca P. Cyclic communication in adaptive strategies to platooning: the case of synchronized merging. *IEEE Trans Intell Veh.* 2020;1. <https://doi.org/10.1109/TIV.2020.3041702>.
35. Rosa MR. Leader-follower synchronization of uncertain Euler-Lagrange dynamics with input constraints. *Aerospace.* 2020;7(9):127.

How to cite this article: Yang K, Liu D, Yu W. A minimal sensing and communication control strategy for adaptive platooning. *Int J Adapt Control Signal Process.* 2022;36:373-390. <https://doi.org/10.1002/acs.3255>